



Rhodium-catalyzed carbonylation of allylaminoalcohols: Catalytic synthesis of *N*-(2-hydroxy-alkyl)-gamma-lactams and bicyclic oxazolidines

J. Limberger^a, M. Mottin^a, F.F. Nachtigall^b, E.E. Castellano^c, R.G. da Rosa^{a,*}

^a Universidade Federal do Rio Grande do Sul, Instituto de Química, Laboratório de Catálise por Metais de Transição, Av. Bento Gonçalves 9500, 91501-970 Porto Alegre, RS, Brazil

^b Universidade Estadual do Rio Grande do Sul, Rua 7 de Setembro 1156, 90010-191 Porto Alegre, RS, Brazil

^c Universidade de São Paulo, Departamento de Física, São Carlos, Av. Trabalhador São-carlense 400, 13566-590 Centro, São Carlos, SP, Brazil

ARTICLE INFO

Article history:

Received 2 June 2008

Received in revised form 8 August 2008

Accepted 12 August 2008

Available online 19 August 2008

Keywords:

Aminoalcohols

Rhodium-carbonylation mechanism

Lactams

Oxazolidines

Limonene

ABSTRACT

Gamma-lactams and bicyclic oxazolidines are important structural frameworks in both synthetic organic chemistry and related pharmacological fields. These heterocycles can be prepared by the rhodium-catalyzed carbonylation of unsaturated amines. In this work, allylaminoalcohols, derived from the aminolysis of cyclohexene oxide, styrene oxide, (*R*)-(+)-limonene oxide, and ethyl-3-phenyl-glicidate, were employed as substrates. These allylaminoalcohols were carbonylated by employing $\text{RhClCO}(\text{PPh}_3)_2$ as a precatalyst under varying CO/H_2 mixtures, and moderate to excellent yields were obtained, depending on the substrate used. The results indicated that an increase in the chelating ability of the substrate ($-\text{OH}$ and $-\text{NHR}$ moieties) decreased the conversion and selectivity of the ensuing reaction. Additionally, the selectivity could be optimized to favor either the γ -lactams or the oxazolidines by controlling the CO/H_2 ratio. A large excess of CO provided a lactam selectivity of up to 90%, while a H_2 -rich gas mixture improved the selectivity for oxazolidines, resulting from hydroformylation/cyclization. Studies of the reaction temperature indicated that an undesirable substrate deallylation reaction occurs at higher temperature ($>100^\circ\text{C}$). Further, kinetic studies have indicated that the oxazolidines and γ -lactams were formed through parallel routes. Unfortunately, the mechanism for oxazolidines formation is not yet well understood. However, our results have led us to propose a catalytic cycle based on hydroformylation/acetalyzation pathways. The γ -lactams formation follows a carbonylation route, mediated by a rhodium-carbamoylic intermediate, as previously reported. To this end, we have been able to prepare and isolate the corresponding iridium complex, which could be confirmed by X-ray crystallographic analysis.

© 2008 Elsevier B.V. All rights reserved.

1. Introduction

Catalytic cyclocarbonylation of allylamines is a well-reported process used to prepare *N*-substituted γ -lactams and pyrrolidines [1–3], where this process has been applied in a number of important fields, such as pharmaceutical research [4–8]. In 1990, Jegorov and co-workers first reported the rhodium-catalyzed carbonylation of *N*-alkylallylamines. In the present work, we have observed a remarkable effect of the quantity of H_2 in the gas mixture, which allows the reaction to be conducted under milder conditions than using pure CO [9]. However, the reaction mechanism remains unclear. In 1996, Da Rosa and Sanchez-Delgado proposed reaction pathways that describe the formation of γ -lactams by rhodium-catalyzed cyclocarbonylation of *N*-alkylallylamines

[1]. In this proposal, γ -lactams are formed by a cyclocarbonylation reaction, where the fundamental step is the nucleophilic attack of the amine nitrogen atom onto a carbonyl group, generating a metal-carbamoyl species. Along with the γ -lactams, non-carbonylated products were also observed, including pyrrolines and pyrrolidines. The origin of these products suggests that reduction of the lactam carbonyl group has taken place by hydrogenation, followed by dehydration (pyrrolines) or dehydration and pyrrolone double bond hydrogenation (pyrrolidines). In agreement with the Jegorov work [9], the authors also observed a promoting effect of H_2 , which they attributed to its role in the formation of the active rhodium-hydride species.

Da Rosa and Buffon suggested that two parallel pathways are operative in the formation of lactams and pyrrolines/pyrrolidines. They proposed that lactams are formed through a rhodium-carbamoyl intermediate, as described above. However, the formation of pyrrolines/pyrrolidines should follow a hydroformylation/cyclization step proceeding through a rhodium-acyl

* Corresponding author. Tel.: +55 5133087318; fax: +55 5133087304.
E-mail address: ricardo.gomes@ufrgs.br (R.G. da Rosa).

intermediate [10]. In order to obtain better selectivity for the γ -lactams, and considering that dehydration is the key step in pyrrolines/pyrrolidines formation, these authors employed a THF/water solvent system to study the reaction. Indeed, under these conditions, the γ -lactam selectivity increased from 40% to 90%. The effect of phosphine ligands on the reaction course was also studied in order to obtain further improvements in the catalytic performance. Using ^{31}P NMR, the authors observed that these ligands were completely oxidized by water under these reaction conditions, explaining the absence of a phosphorus ligand effect on the catalytic behavior. Therefore, this suggested that water could replace the phosphines as a ligand in the catalytic process, increasing the selectivity for γ -lactams [11].

The carbonylation/hydroformylation of *N,O*-functionalized alkenylamines can produce both lactams and/or fused heterocycles [12–14]. Jackson and co-workers have studied the carbonylation of *N*-alkenyl-1,3-diaminopropanes (alkenyl=allyl or 3-butenyl), which provided fused diazabicycloalkanes and lactams. Selectivity control was achieved by carefully optimizing the gas mixture. As such, a large excess of CO ($\text{CO}/\text{H}_2 = 9/1$) favored carbonylation, while an excess of H_2 ($\text{CO}/\text{H}_2 = 1/9$) provided primarily the products of hydroformylation. The phosphine ligand effect on the selectivity was also studied, using ligands bearing different steric hindrances and Lewis basicity. Neither the steric demand nor the Lewis basicity of monodentate ligands presented a clear relationship to the hydroformylation or carbonylation products selectivity. However, chelating phosphines, such as BIPHEPHOS, led to the hydroformylation product selectively. Similar results were reported in the carbonylation of isopropylallylamine and *n*-butylallylamine, these being attributed to the difficulty in the formation of the rhodium–carbamoyl intermediate imposed by the chelating metal–ligand ring [12]. Considering the selectivity obtained using chelating phosphines, Jackson and co-workers recently reported the preparation of diazabicycloalkanes and oxazabicycloalkanes from the hydroformylation of 1,3-diaminopropanes and *N*-alkenylaminethanols [13,14].

In the present work, we have studied the carbonylation of allylaminoalcohols, used to prepare *N*-(2-hydroxy-alkyl)- γ -lactams and oxazolidines. We discuss our efforts to control reaction selectivity, and subsequently rationalize a mechanism for the selective formation of both γ -lactams and oxazolidines. Our approach (Scheme 1) was based on the aminolysis of the following epoxides: cyclohexene oxide, **1**; styrene oxide, **2**; (*R*)-(+)-limonene oxide, **3**; hydrogenated (*R*)-(+)-limonene oxide, **4** and the ethyl-3-phenylglycidate **5**. The aminoalcohols obtained were subsequently carbonylated, providing γ -lactams and oxazolidines as the primary products. We further discuss the influence of the hydroxyl group, and the nucleophilicity of the nitrogen in the ring-closing process. Finally, a catalytic cycle that explains the formation of the obtained oxazolidines is proposed.

2. Experimental

2.1. Materials

$\text{RhCl}(\text{CO})(\text{PPh}_3)_2$ was prepared as described in literature [15]. THF (Nuclear, P.A.) was distilled over Na/benzophenone under an argon atmosphere. Water was distilled before use. Carbon monoxide (White Martins, 99.5%), hydrogen (White Martins, 99.999%), allylamine (Aldrich, 98%), cyclohexene oxide (Aldrich), styrene oxide (Aldrich), ethyl-3-phenylglycidate (Aldrich) and (*R*)-(+)-limonene-oxide (Aldrich, 97%, mixture of *cis* and *trans*) were used as received. Vaska's complex ($\text{IrCl}(\text{CO})(\text{PPh}_3)_2$) (Strem) was used as received.

2.2. Aminoalcohols synthesis

Aminoalcohols **1a**, **2a**, **3a**, and **4a** were prepared by an adaptation of the method described by Singaram et al. [16,17]. In a typical experiment, 20 mmol of epoxide, 40 mmol of allylamine, and 30 mmol of water were added to a screw-top schlenk flask. The flask was heated to 80 °C, stirred with magnetic stirbar for 24 h, and purified by acid/base extraction. Allylaminoalcohol **5a** was prepared according to the following protocol: A glass flask was used, to which was added 10 mmol of ethyl-3-phenyl-glycidate, 10 mmol of allylamine, and 50 mL of ethanol. The resulting solution was refluxed for 24 h at 80 °C. Next, the solvent was evaporated, and the product was purified by column chromatography using hexane/ethyl acetate as eluent. The silanization was performed as described in literature [18].

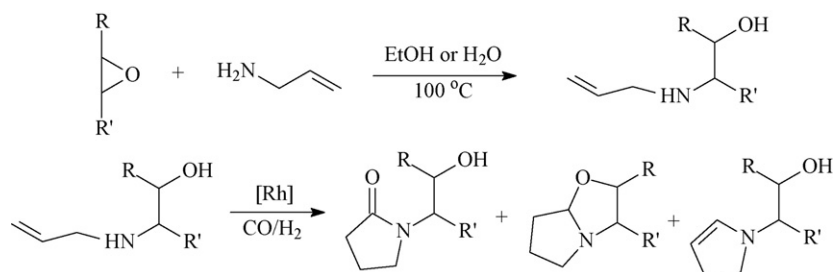
2.3. Catalytic experiments

Catalytic experiments were performed in a 100 mL stainless steel reactor under 20 or 40 bar with varying $\text{CO}:\text{H}_2$ ratios. The reaction temperature was maintained at 50, 70, or 100 °C, and the solution was stirred with a magnetic stirbar for 24 h. In a typical experiment, 3.00 mmol aminoalcohol (or protected aminoalcohol), 0.015 mmol $\text{RhCl}(\text{CO})(\text{PPh}_3)_2$, and 20 mL THF were added to a schlenk flask and then transferred *via* cannula to the stainless steel reactor under an argon atmosphere. The reactor was closed, purged with CO, pressurized, and heated in a silicon oil bath at 50 °C. The products were analyzed by GC, GC–MS and purified using column chromatography.

All the isolated products were further analyzed by MS, IR and NMR techniques. The detailed spectroscopy results are available in [supplementary material file](#).

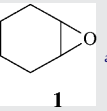
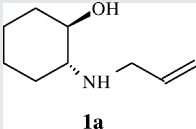
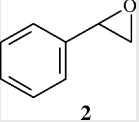
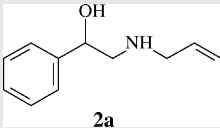
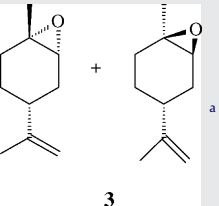
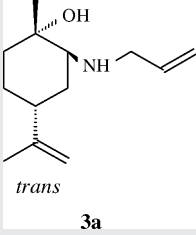
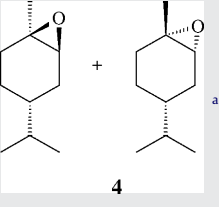
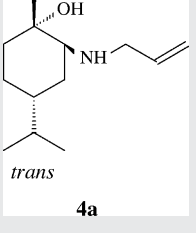
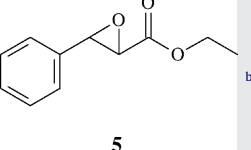
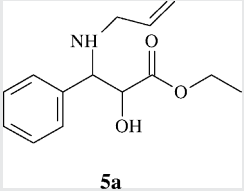
2.4. Iridium–carbamoyl complex synthesis

The iridium analogs for the rhodium–carbamoyl intermediate was synthesized reacting 0.32 mmol (250 mg) of the Vaska's Complex ($\text{IrCl}(\text{CO})(\text{PPh}_3)_2$) with 16.02 mmol of isopropylallylamine



Scheme 1. Aminolysis of the epoxides followed by allylaminoalcohols carbonylation.

Table 1
Results of epoxides aminolysis and aminoalcohol structures

Epoxide	Conversion (%)	Selectivity (%)	Aminoalcohol
	100	100	
	100	100	
	55	100	
	52	100	
	80	90 ^c	

^a Allylamine, H₂O, 80 °C, 18–24 h.

^b Allylamine, EtOH reflux, 22 h.

^c 10% diallylated by-product.

(1.6 g) in a 100 mL stainless steel reactor, under 10 bar of CO/H₂ (4/1), in 15 mL of anhydrous THF at 70 °C for 12 h. Next, the reactor was cooled at room temperature, vented and the reaction mixture was concentrated to the half of its volume. The resulting solution was filtered through Celite in order to eliminate ammonium salt and phosphine oxide. The filtrate was evaporated to dryness and the residue was washed (3 × 5 mL) with pentane resulting in a white micro-crystalline powder. This product was further purified by recrystallization from THF/ethyl ether at –6 °C, affording 82 mg (40% yield).

2.5. X-ray crystallographic study

Crystallographic data (excluding structure factors) for the structure reported in this paper have been deposited with the Cambridge Crystallographic Data Centre as supplementary publication no. CCDC-625739. Copies of the data can be obtained free of charge on application to CCDC, 12 Union Road, Cambridge CB2 1EZ, UK [Fax: int. code + 44 (1223) 336-033; E-mail: deposit@ccdc.cam.ac.uk]. Crystal data, their collection

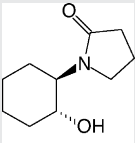
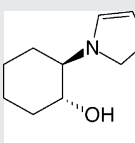
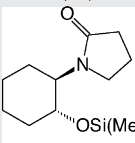
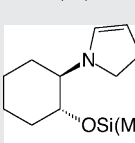
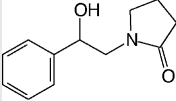
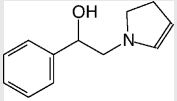
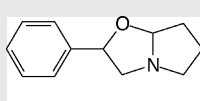
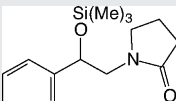
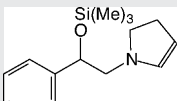
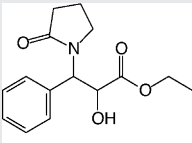
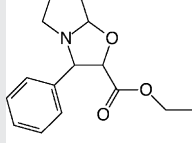
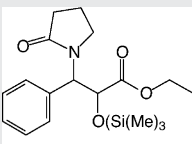
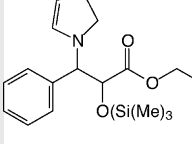
details and software refinements are supplied as **supplementary material**.

3. Results and discussion

3.1. Epoxide aminolysis

The aminolysis reactions were carried out as reported by Singaram et al. who used water as a promoter for the reaction [16,17]. Under the reaction conditions employed herein, cyclohexene oxide and styrene oxide were fully converted into the aminoalcohols **1a** and **2a**, respectively (Table 1). As previously observed by Singaram, the *trans* diastereomer of the commercial mixture (*cis/trans*) of limonene oxide was selectively converted to the *trans* aminoalcohol **3a** as the *cis* diastereomer did not react and could be isolated for further reactions. The same behavior was observed for the hydrogenated limonene oxide affording the *trans* aminoalcohol **4a** in high isolated yield. In order to obtain the allylaminoalcohol **5a**, it was necessary to use ethanol instead of water as the solvent in order

Table 2
Results and products of the aminoalcohols carbonylation

Entry ^a	Substrate	Conversion (%)	γ -Lactam	Hydroformylation products (%)		Other products (%)
				Pyrroline	Oxazolidine	
1	1a	54	 1b (50)	 1c (33)	–	12
2	1a'	88	 1b' (63)	 1c' (24)	–	13
3	2a	95	 2b (36)	 2c (23)	 2d (28)	13
4	2a'	99	 2b' (69)	 2c' (18)	–	13
5	3a	100	–	–	–	100
6	5a	95	 5b (31)	–	 5d (69)	–
7	5a'	81	 5b' (33)	 5c' (67)	–	–

RhClCO(PPh₃)₂, THF, 20 bar CO/H₂ (4/1), 50 °C, 24 h, substrate/Rh = 200.

^a Average of 3 runs. Other products: hydrogenation, deallylation, isomerization and heavy products.

to avoid the aminolysis of the ester moiety of the ethyl-3-phenylglycidate.

3.2. Carbonylation of allylaminoalcohols

The results of preliminary studies on carbonylation of the synthesized allylaminoalcohols are presented in Table 2. The reaction conditions were the same as those reported in literature for the case of the alkylallylamine carbonylation [3,10,11]. Indeed, under these conditions, the desired product was obtained with high conversion, with substrate **1a** being the only exception. This can be explained by considering the stability of the chelate formed between this cyclohexene-derived β -aminoalcohol and the rhodium, resulting from the rigidity of the cyclohexene carbon ring. In order to prevent chelate formation, the hydroxyl group of **1a** was protected as the silyl ether. Gratifyingly, the protection of the hydroxyl group led to

better conversion (entry 2), supporting our hypothesis. In the case of **3a**, only a complex mixture of heavy products was observed, despite the high reactivity of the substrate (entry 5). This likely occurs due to the hydroformylation of isopropenyl group, generating a formyl functionality that can be subsequently attacked by the amine group of the other molecule.

The selectivity of the reaction for the γ -lactam formation followed the order: **1a** > **2a** > **5a**. This order correlates well with the basicities of the nitrogen atoms in each molecule [19], and is in a good agreement with previous reports for alkylallyl amines [10].

Other noteworthy products observed included five-membered fused bicyclic oxazolidines **2d** and **5d**. Jackson and co-workers have reported analogous compounds with larger rings (typically 8–13 members) formed by a hydroformylation/cyclization sequence [13,14]. In contrast to the proposition that the rhodium species

are involved only in the hydroformylation process, we suggest that the oxazolidine formation occurs entirely inside the coordination sphere of the catalyst.

The hydroxyl silanization of substrates **1a** and **2a** affected both the conversion and the selectivity toward γ -lactam formation. The improvement in the γ -lactam selectivity can be rationalized by the better availability of the nitrogen non-bonding electron pair due to the lack of an intramolecular hydrogen bond. In fact, our previous results indicated that the higher electron density on nitrogen, the higher the γ -lactam yield [10]. On the other hand, the silanization did not produce significant effect on the γ -lactam selectivity in the case of **5a** and **5a'**, likely due to the intrinsic low electron density on the nitrogen atom, resulting in competing hydroformylation with these substrates.

3.2.1. Carbonylation of **1a** and **1a'**

In order to improve the conversion of aminoalcohol **1a**, harsher reaction conditions were considered (Table 3). By increasing the pressure, the conversion was increased from 54% (entry 1) to 95% (entry 3). However, the lactam selectivity remained nearly the same. Further temperature increases led to a higher yield in substrate deallylation product (entries 4 and 5), allowing us to confirm and characterize the 2-aminocyclohexanol product (Fig. 1). As reported earlier in the literature, the presence of water in the solvent at 100 °C sometimes improves lactam selectivity [11]. However, under these conditions (entry 6), the desired pyrroline reduction was not observed, but rather an unexpected decrease in the substrate deallylation took place, despite the high temperatures.

It has been previously reported that rhodium systems modified with $P(o\text{-tol})_3$ provide γ -lactams with high selectivity in the carbonylation of *N*-alkenyl-1,3-diaminepropanes [12]. In direct contrast to these results, entries 7 and 8 showed a very low and no conversion, respectively. This ligand likely hindered aminoalcohol coordination to the active site of the rhodium catalyst. Another variable that has been shown to modulate selectivity is the CO/H₂

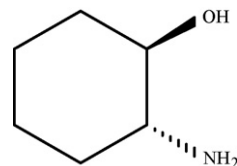


Fig. 1. Aminoalcohol **1a** deallylation by-product.

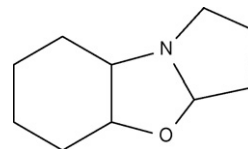
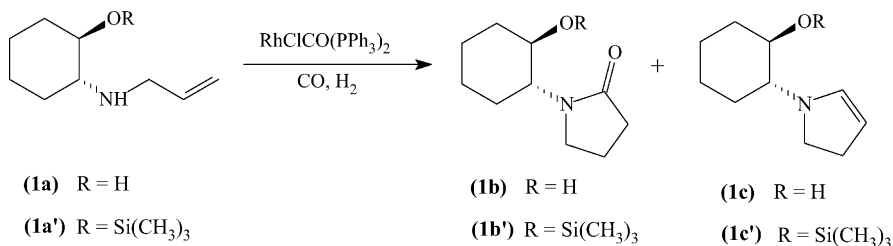


Fig. 2. Constrained tricyclic-oxazolidine, generated from **1a**.

ratio [12]. In fact, a CO/H₂ ratio of 9/1 (entry 9) provided 98% conversion and 90% selectivity for the lactam under otherwise identical reaction conditions. On the other hand, enrichment in hydrogen (CO/H₂ = 1/4) led primarily to hydroformylation (entry 10). While both pyrroline and oxazolidine products were expected under the latter conditions, only pyrroline **1c** was observed. This is likely due to the ring strain imposed by the constrained fused rings of the tricyclic-oxazolidine, as shown in Fig. 2. In order to improve carbonylation selectivity, we employed the hydroxyl-protected substrate **1a'** and a CO rich gas mixture (entry 11). Indeed, under these conditions we obtained a higher yield in γ -lactam (93%). A drawback in using a high CO/H₂ ratio is the reaction time, which is significantly increased due to catalyst poisoning by CO.

Table 3
Results of **1a** and **1a'** carbonylation



Entry	Substrate	<i>T</i> (°C)	<i>P</i> (bar) (CO/H ₂)	Conversion (%)	γ -Lactam (%)	Pyrroline (%)	Deallylation (%)	Other products (%)
1	1a	50	20 (4/1)	54	50	33	6	11
2	1a'	50	20 (4/1)	88	63	24	6	7
3	1a	50	40 (4/1)	95	52	33	5	10
4	1a	70	40 (4/1)	91	38	40	12	10
5	1a	100	40 (4/1)	90	40	5	45	10
6	1a	100	40 (CO/H ₂ O) ^a	89	46	10	36	8
7 ^b	1a	50	40 (4/1)	17	55	31	7	7
8 ^c	1a	50	40 (4/1)	0	–	–	–	–
9 ^d	1a	50	40 (9/1)	98	90	5	–	5
10	1a	50	40 (1/4)	85	32	53	6	9
11 ^d	1a'	50	20 (9/1)	99	94	6	–	–

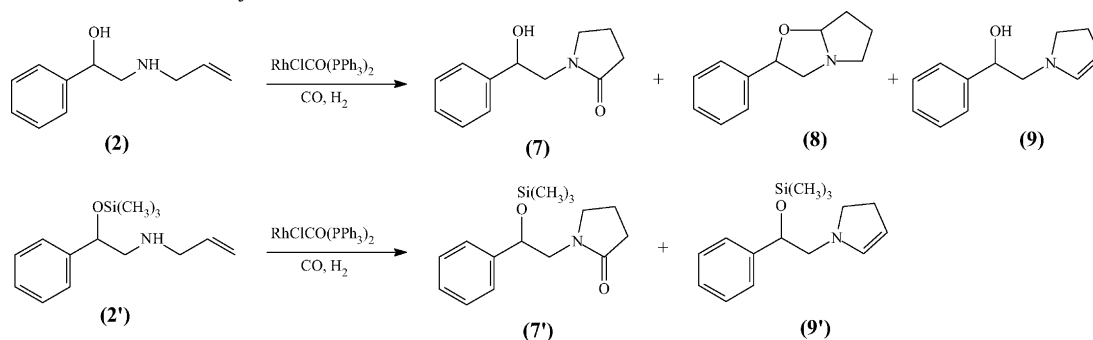
RhClCO(PPh₃)₂, THF, 24 h, substrate/Rh = 200; other products: hydrogenation, isomerization and heavy products.

^a 23% (v/v) H₂O/THF.

^b [RhCl(CO)₂]₂, *P*(*o*-tol)₃ *P*/Rh = 2.

^c RhCl₃·3H₂O, *P*(*o*-tol)₃ *P*/Rh = 2.

^d 48 h.

Table 4
Results of **2a** and **2a'** carbonylation

Entry	Substrate	<i>t</i> (h)	<i>P</i> (bar) (CO/H ₂)	Conversion (%)	Pyrroline (%)	Oxazolidine (%)	γ-Lactam (%)	Other products (%)
1	2a	24	20 (4/1)	95	23	28	36	13
2	2a'	24	20 (4/1)	99	18	–	69	13
3 ^a	2a	24	40 (4/1)	12	23	26	38	13
4	2a	24	20 (1/1)	94	21	38	21	20
5	2a	24	20 (1/4)	93	26	59	10	5
6	2a	48	20 (9/1)	90	13	24	50	13
7	2a'	24	20 (9/1)	64	10	–	86	4
8	2a'	48	20 (9/1)	98	9	–	88	3

RhClCO(PPh₃)₂, THF, 50 °C, substrate/Rh = 200. Other products: hydrogenation, isomerization and heavy products.

^a [RhCl(CO)₂]₂, tri-*o*-toluylphosphine.

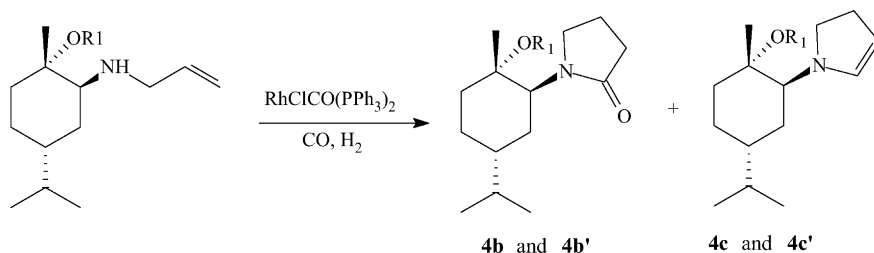
3.2.2. Carbonylation of **2a** and **2a'**

Substrate **2a** provided high conversion even under the milder conditions tested (Table 4, entry 1). The selectivity control was achieved using the same procedure as employed to **1a**, i.e., phosphine catalyst modulation, CO/H₂ composition, and substrate silanization (**2a'**). The results using *P*(*o*-Tol)₃ as ligand are presented in entry 3. As observed above (Table 2, entry 7), the conversion was low even at 40 bar, supporting our hypothesis that this phosphine blocks substrate coordination. As seen for **1a**, the higher the H₂ in the gas composition, the higher the hydroformylation yield (entries 4 and 5). It is noteworthy that, for this substrate, we also observed formation of oxazolidine **2c**. Its formation can be rationalized by the less constrained bicyclic system compared to the analogous system

derived from **1a** (Fig. 2). The lactam yield was improved by enrichment of CO in the gas mixture, but again, this protocol requires a longer reaction time (entry 6). Upon the silanization of **2a**, a remarkable improvement in the lactam selectivity was observed (entries 7 and 8), as expected.

3.2.3. Carbonylation of **3a**, **4a** and **4a'**

As discussed above, carbonylation of **3a** led to a complex mixture of heavy products due to the hydroformylation of both isopropenyl and allyl double bonds. In order to overcome this problem, we attempted to run the reaction under water-gas-shift conditions (CO/H₂O, 100 °C). Unfortunately, the main product observed was that of substrate deallylation.

Table 5
Results of **4a** and **4a'** carbonylation

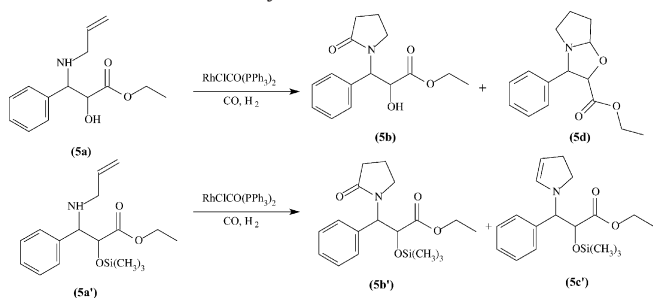
4a : R = H

4a' : R = Si(CH₃)₃

Entry	Substrate	<i>t</i> (h)	<i>T</i> (°C)	CO/H ₂	Conversion (%)	Pyrroline (%)	γ-Lactam (%)	Isomerization (%)	Deallylation (%)
1	4a	24	50	(4/1)	41	67	15	14	4
2	4a	24	70	(4/1)	74	56	6	17	21
3	4a	48	50	(4/1)	93	65	17	13	5
4	4a	24	50	(9/1)	25	44	34	15	7
5	4a	48	50	(9/1)	60	46	33	16	5
6	4a	48	70	(1/4)	85	73	9	6	12
7	4a'	48	50	(9/1)	88	44	35	16	5

RhClCO(PPh₃)₂, 40 bar CO/H₂, THF, substrate/Rh = 200.

Table 6
Results of the **5a** and **5a'** carbonylation



Entry	Substrate	<i>t</i> (h)	<i>P</i> (bar) (CO/H ₂)	Conversion (%)	Oxazolidine (%)	Pyrroline (%)	γ-Lactam (%)
1	5a	24	20 (4/1)	95	69	–	31
2	5a'	24	20 (4/1)	81	–	67	33
3	5a	24	20 (1/1)	100	88	–	12
4	5a	24	20 (1/4)	97	95	–	5
5	5a	48	20 (9/1)	95	47	–	53
6	5a'	48	20 (9/1)	93	–	44	56

RhClCO(PPh₃)₂, THF, 24 h; 50 °C. Substrate/Rh = 200.

The most direct way to avoid the heavy products is through hydrogenation (Pd/C, 5%, 95% isolated yield) of the limonene oxide isopropenyl group. The hydrogenated substrate **4a**, was thus subjected to the carbonylation conditions, and the results are presented in Table 5. Considering the increased steric hindrance of **4a**, the reactions were run at an increased pressure of 40 bar, providing only relatively low conversion (41%, entry 1). Increasing the temperature to 70 °C resulted in a concomitant increase in conversion to 74%, however at the expense of lactam and pyrroline selectivity due to increased substrate deallylation (entry 2). Maintaining the temperature at 50 °C for 48 h, the deallylation was minimized and the conversion was improved to 93%. Unfortunately, the γ-lactam selectivity remained low (entry 3). In order to improve the carbonylation, a CO/H₂ ratio = 9/1 was employed, providing a better lactam selectivity, but a lower conversion (entries 4 and 5). Under these conditions, the oxazolidine was not formed, as observed for **1a**, even at a CO/H₂ ratio of 1/4 (entry 6), reinforcing the importance of the strain in the polycyclic ring system in this product. Again, substrate silanization (**4a'**) provided only an improvement in conversion, as discussed for **1a** (entry 7).

3.2.4. Carbonylation of **5a** and **5a'**

The results for the carbonylation of **5a** and **5a'** are presented in Table 6. As previously described, the reaction conditions were adjusted to provide either hydroformylation or carbonylation products. By employing H₂ in excess, oxazolidine **5d** was obtained in a high yield (entries 3 and 4), while with excess of CO, γ-lactam selectivity was increased from 30% (entries 1 and 2) to 50% (entries 5 and 6) for both **5a** and **5a'**.

3.3. Mechanistic studies for oxazolidine and γ-lactam formation

3.3.1. Oxazolidines

Silanization of aminoalcohols **2a** and **5a** has allowed us to rationalize whether oxazolidine formation follows the hydroformylation/cyclization pathway or the carbonylation pathway. The carbonylation of silylated substrate **2a'** led to the expected suppression of oxazolidine formation, accompanied with a modest increase in the lactam yield (Table 2, entries 3 and 4). This suggests that the oxazolidine is formed through the carbonylation pathway, with the lactam as a precursor.

Indeed, prior studies have described the formation of oxazolidines from the reductive cyclization of hydroxy-lactams [20].

On the other hand, in the carbonylation of protected substrate **5a'**, the selectivity for lactam remained nearly constant (Table 2, entry 7). Additionally, pyrroline was observed as a new product, being formed with the same selectivity as the corresponding oxazolidine in the case of **5a** carbonylation (Table 2, entry 6). This strongly implies that the oxazolidine is not formed through the lactam path in this case, but rather through a hydroformylation mechanism.

In order to further clarify the observations made regarding oxazolidine formation, a kinetic study of aminoalcohol **2a** carbonylation (taken as standard) was conducted. The data outline in Fig. 3 indicates that the selectivity for γ-lactams, pyrroline, and oxazolidine remains nearly constant along the reaction coordinate. This strongly suggests that γ-lactam is formed through a parallel mechanism, as discussed above. However, as pyrroline is always formed in a lower yield than the corresponding oxazolidine, they

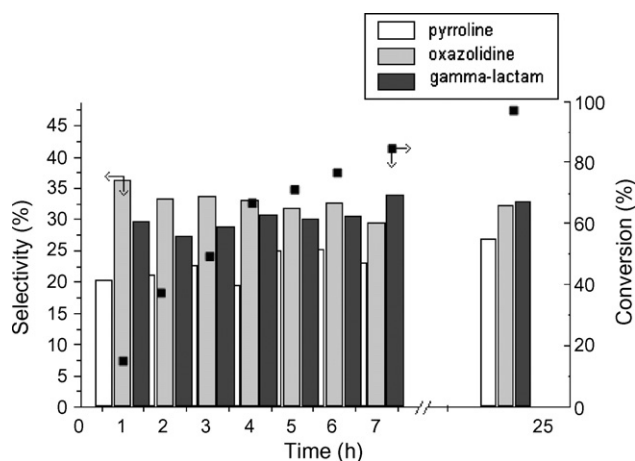


Fig. 3. Selectivity profile for lactam **2b**, pyrroline **2c**, and oxazolidine **2d** during the carbonylation of **2a**. Reaction conditions: RhClCO(PPh₃)₂ (0.5 mol%), THF, CO/H₂ = 4, *P* = 20 bar (kept constant during the reaction), **2a**/Rh = 200.

likely share some steps in common in their mechanisms of formation.

Based on the mechanistic observations discussed above, we propose that the oxazolidine is formed through the catalytic cycle illustrated in Fig. 4. The first step is substrate coordination to the rhodium catalysts, forming the chelate (B). Next, hydrogen insertion takes place, generating the saturated metallacycle (C), which is subsequently replaced by the acyl-complex (D), upon CO insertion. The carbonyl group in the intermediate (D) should suffer intramolecular attacks from both the hydroxyl (generating (E)) and the amine groups. Hydrogenation and elimination of water provides complex (F). The product and the catalytically active species (A) are finally released from (F) after reductive elimination, along with CO insertion.

To the best of our knowledge, this is the first proposed catalytic cycle for this transformation. Until now, the formation of oxazolidines from hydroformylation reactions has been explained by the following steps: (i) olefin hydroformylation; (ii) secondary amine fragment attack of the carbonyl of the resulting aldehyde, forming an iminium ion; (iii) iminium ion attack by the nucleophilic hydroxyl group [12–14]. The first two steps occur outside the coordination sphere of the rhodium species. However, it was also reported that a phosphorus ligand could drive the selectivity for cyclic (intramolecular condensation) or polymeric products (intermolecular condensation) [13,14]. In light of these observa-

tions and the results described above, it is more likely that the true mechanism for oxazolidine formation involves only metal-complex mediated steps, as described in our proposal. Moreover, the first order dependence on the substrate (Fig. 5) indicates that coordination of the substrate to the active catalyst (A), generating intermediate (B), would be involved in a pre-equilibrium or in the rate-limiting step. This result is in accord with the proposed catalytic cycle, where most of the mechanistic steps occur inside the rhodium coordination sphere, and are therefore expected to be fast.

3.3.2. γ -Lactams

The lactams obtained from the allylaminoalcohols are formed by the same mechanism described for *N*-alkyl-allylamines. The key step is the formation of a rhodium–carbamoyl species generated by nucleophilic attack of the amine moiety of the substrate to a metal–carbonyl group [3]. Iridium analogs of this carbamoylic compound have been isolated and characterized previously. However, we were recently able to obtain an X-ray crystal structure of this compound, as presented in Fig. 6 and Table 7, confirming structure and connectivity.

This complex has been previously prepared by reacting Vaska's complex ($\text{IrCl}(\text{CO})(\text{PPh}_3)_2$) with isopropylallylamine, affording the product as colorless bricks. This metallacycle released the corresponding *N*-isopropyl- γ -lactam when heated to 50 °C under

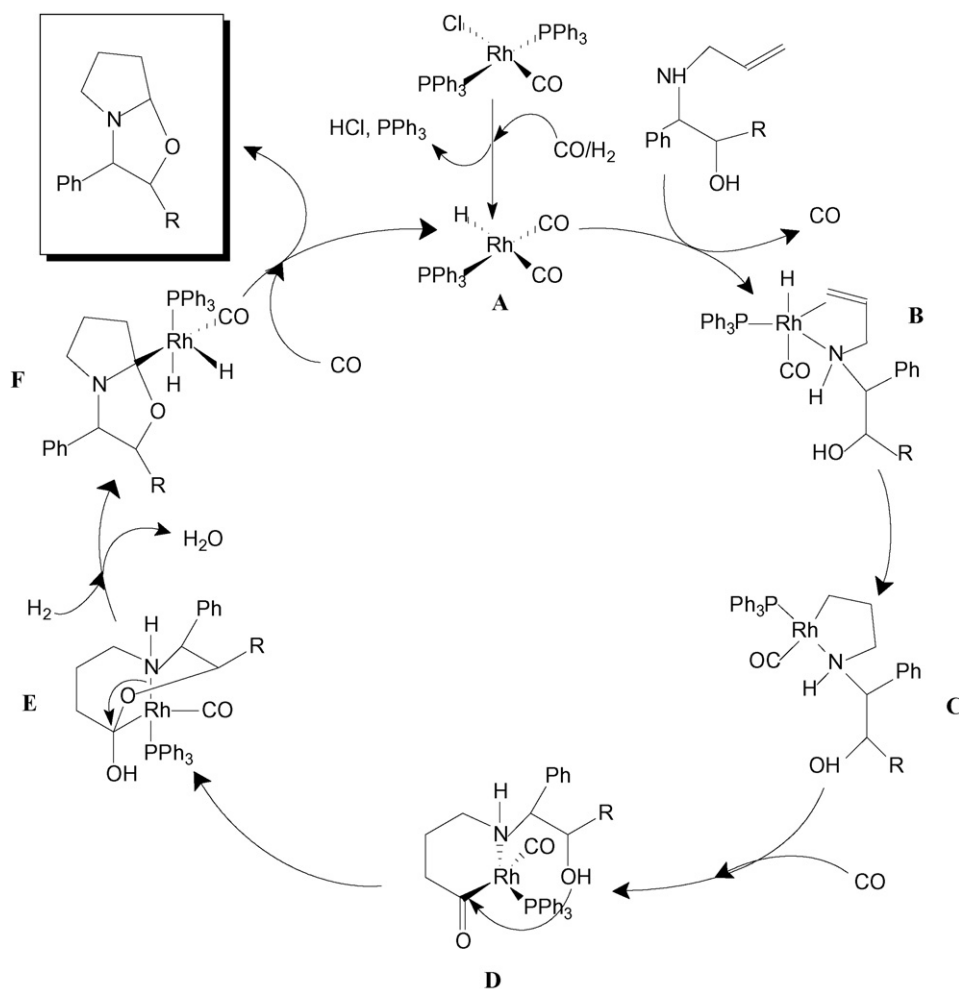


Fig. 4. Proposed catalytic cycle for bicyclic oxazolidines formation.

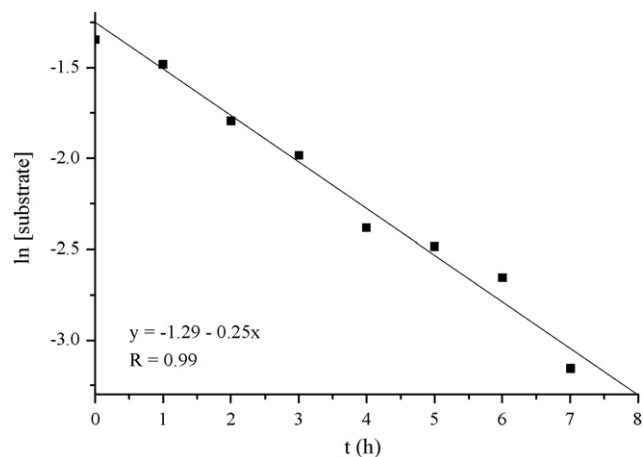


Fig. 5. Kinetic effect of the substrate concentration on the rate of **2a** carbonylation.

20 bar of H₂ [10]. This complex could be assigned as either a trigonal bipyramidal or a distorted octahedral structure (Fig. 6). From Table 8, it is possible to verify that the Ir1–PPh₃ bond is longer than that reported for the trigonal bipyramidal complex *trans*-Ir(PPh₃)₂(CO)₂Cl (2.33 Å) [21]. This is likely due to a degree of electronic repulsion between the phenyl ring of the PPh₃ ligand and the coordinated allylamine double bond. The P1–Ir1–C13 angle displays some deviation from linearity (174.1°) probably due to metallacycle ring strain. The bond order between iridium and the double bond carbons (C10 and C11) is also different, making the geometry of the complex more octahedron-like. The bond order is greater for Ir1–C11 than for Ir1–C10, as shown by the differences in both their bond lengths and bond angles Ir1–C11–C13 and Ir1–C10–C13. This bond order dif-

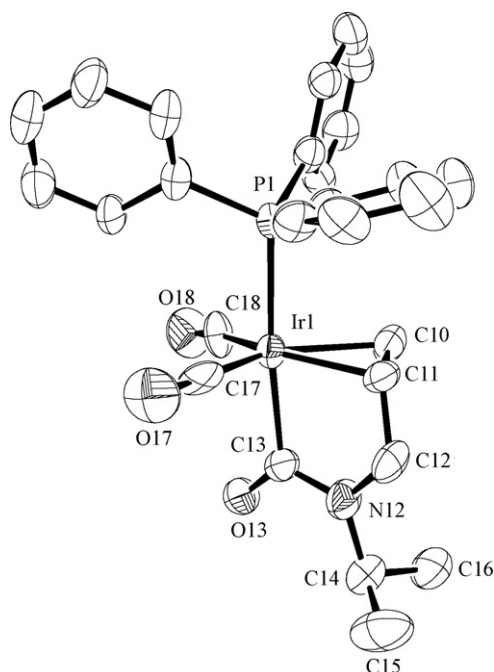


Fig. 6. Ortep diagram for the iridium-carbamoyl complex with 50% probability thermal ellipsoids.

Table 7
Crystal data and structure refinement

Empirical formula	C ₂₇ H ₂₇ IrNO ₃ P
Formula weight	636.67
Temperature	296(2) K
Wavelength	0.71073 Å
Crystal system	Triclinic
Space group	P-1, #2
Unit cell dimensions	$a = 11.971(2)$ Å, $\alpha = 91.000(10)^\circ$ $b = 12.346(2)$ Å, $\beta = 90.660(10)^\circ$ $c = 17.635(2)$ Å, $\gamma = 103.690(10)^\circ$
Volume	2531.6(7) Å ³
Z	4
Density (calculated)	1.668 Mg/m ³
Absorption coefficient	5.365 mm ⁻¹
Absorption correction	Numerical
Max./Min. transmission	0.5661/0.3836
F(0 0 0)	1244
Crystal size	0.089 mm × 0.133 mm × 0.205 mm
Theta range for data collection	2.71–26.00°
Index ranges	–14 ≤ h ≤ 14, –15 ≤ k ≤ 15, –21 ≤ l ≤ 21
Reflections collected	16,420
Independent reflections	9291 [R(int) = 0.0866]
Completeness to theta = 26.00°	93.3%
Refinement method	Full-matrix least-squares on F ²
Data/restraints/parameters	9291/0/599
Goodness-of-fit on F ²	1.022
Final R indices [I > 2σ(I)]	R ₁ = 0.0438, wR ₂ = 0.0866
R indices (all data)	R ₁ = 0.0883, wR ₂ = 0.1046
Largest diff. peak and hole	1.696 and –2.100 e Å ⁻³

ference results in different *trans* influences, which make the Ir1–C18 longer than Ir1–C17. The stronger bond between Ir1–C11 (relative to Ir1–C10) is expected when considering the greater electron density over C11, provided by the carbon chain attached to it.

Fig. 7 presents our proposed catalytic cycle for allylminoalcohol carbonylation, to provide γ -lactams. The catalytic species (A) is formed by PPh₃ substitution for a CO ligands, oxidative addition of H₂, and reductive elimination of HCl. Next, nucleophilic attack of the amine moiety of the allylminoalcohol to a rhodium-carbonyl group takes place, providing an unsaturated carbamoyl-metallacycle (B). After a hydride insertion, the intermediate (C) is formed. Finally, by a reductive elimination step together with a concomitant CO coordination, lactam (D) and catalyst (A) are produced.

Table 8
Selected bond distances and angles for the iridium-carbamoyl complex with estimated standard deviation in parenthesis

Bond	Length (Å)	Bond	Angle (°)
Ir1–P1	2.390(3)	P1–Ir1–C13	174.1(3)
Ir1–C18	1.906(11)	C18–Ir1–C17	109.6(5)
Ir1–C17	1.883(3)	C18–Ir1–C13	90.3(5)
Ir1–C13	2.117(12)	C17–Ir1–C13	89.2(5)
Ir1–C11	2.149(12)	C11–Ir1–C13	79.3(5)
Ir1–C10	2.182(11)	C10–Ir1–C13	84.9(5)
C10–C11	1.435(17)	C10–Ir1–C11	38.7(5)
C13–O13	1.207(14)	C10–Ir1–C18	107.3(5)
C17–O17	1.179(15)	C11–Ir1–C17	104.1(5)
C18–O18	1.150(14)	Ir1–C13–N12	112.0(9)
C12–N12	1.436(15)	Ir1–C11–C12	110.2(8)
C13–N12	1.377(15)		
C14–N12	1.476(16)		

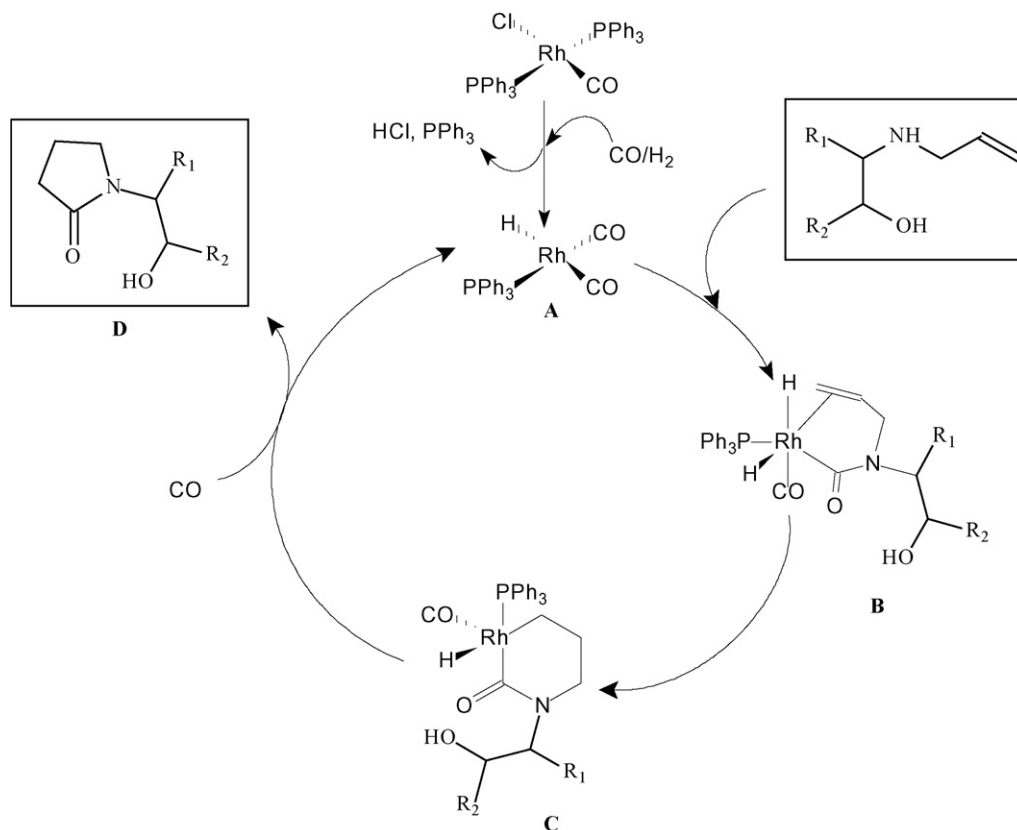


Fig. 7. Proposed catalytic cycle for the rhodium-catalyzed allylaminoalcohol carbonylation to afford *N*-(2-hydroxy-alkyl)- γ -lactams.

4. Conclusions

The catalytic reactions studied herein provide access to valuable products arising from both hydroformylation (oxazolidines) and carbonylation (γ -lactams). The selectivity control for these products was achieved by tuning the CO/H₂ molar ratio. A high CO concentration drove the selectivity toward the lactam, while the oxazolidines were the main product when a H₂-rich gas mixture was employed. The chelating ability of β -allylaminoalcohols has shown a negative effect on the reactivity. This problem was overcome by the selective protection of the substrate hydroxyl group as the TMS ether.

Experimental evidences suggest that the oxazolidines are formed through hydroformylation of the allylaminoalcohol double bond, followed by consecutive intramolecular attack of the amine and hydroxyl groups to the metal-acyl intermediate. In studying the mechanism of γ -lactam formation, we obtained the X-ray crystal structure of an iridium-carbamoyl complex prepared under the same reaction conditions used for the rhodium-catalyzed reaction. This achievement provides indirect support for our assumption that the key step of the mechanism is the formation of a metal-carbamoyl intermediate.

Acknowledgments

We would like to thank Prof. J. Dupont and Prof. A.L. Monteiro for GC-MS facilities and valuable mechanistic discussions. J. Limberger gratefully acknowledges the CAPES for the scholarship.

Appendix A. Supplementary data

Supplementary data associated with this article can be found, in the online version, at doi:10.1016/j.molcata.2008.08.005.

References

- [1] J. Falbe, *Angew. Chem. Int. Ed. Engl.* 5 (5) (1966) 435.
- [2] J.F. Knifton, *J. Organomet. Chem.* 188 (1980) 223.
- [3] R.A. Sánchez-Delgado, R.G. da Rosa, E. Ocando-Mavarez, *J. Mol. Catal. A: Chem.* 108 (1996) 125.
- [4] K.K. Gandhi, C.R. Bidhan, S.D. Adhikari, J.K. Ray, N.K. Brahma, *Bioorg. Med. Chem.* 6 (1998) 2397.
- [5] K. Dolbeare, G.F. Pontoriero, S.K. Gupta, R.K. Mishra, R.L. Johnson, *J. Med. Chem.* 46 (2003) 727.
- [6] J.J.W. Duan, L. Chen, Z.R. Wasserman, L. Zhonghui, R.Q. Liu, M.B. Covington, M. Qian, K.D. Hardman, R.L. Magolda, R.C. Newton, D.D. Christ, R.R. Wexler, C.P. Decicco, *J. Med. Chem.* 45 (2002) 4954.
- [7] J.C. Pelletier, J. Rogers, J. Wrobel, M.C. Perez, E.S. Shen, *Bioorg. Med. Chem.* 13 (2005) 5986.
- [8] M. Matsukawa, T. Hirai, S. Karita, T. Akizawa, H. Pan-Hou, M. Yoshioka, G. Goto, H. Parvez, M.B.H. Youdim, *Neurotoxicology* 25 (2004) 293.
- [9] A. Jegorov, T. Trnka, F. Turecek, V. Hanus, *J. Mol. Catal. A Chem.* 63 (1990) 335.
- [10] R.G. da Rosa, J.D. Ribeiro de Campos, R. Buffon, *J. Mol. Catal. A: Chem.* 137 (1999) 297.
- [11] R.G. da Rosa, J.D. Ribeiro de Campos, R. Buffon, *J. Mol. Catal. A: Chem.* 153 (2000) 19.
- [12] D.J. Bergmann, E.M. Campi, W.R. Jackson, Q.J. McCubbin, A.F. Patti, *Tetrahedron* 53 (1997) 17449.
- [13] D.J. Bergmann, E.M. Campi, W.R. Jackson, A.F. Patti, *Chem. Commun.* (1999) 1279.
- [14] D.J. Bergmann, E.M. Campi, W.R. Jackson, A.F. Patti, *Aust. J. Chem.* 52 (1999) 1131.
- [15] D. Evans, J.A. Osborn, G. Wilkinson, *Inorg. Synth.* 11 (1968) 99.

- [16] B. Singaram, W. Chrisman, J.N. Camara, K. Marcellini, C.T. Goralski, D.L. Hasha, P.R. Rudolf, L.W. Nicholson, K.K. Borodychuk, *Tetrahedron Lett.* 42 (2001) 5805.
- [17] B. Singaram, D. Steiner, L. Ivison, C.T. Goralski, R.B. Appel, J.R. Gojkovick, *Tetrahedron Asymm.* 13 (2002) 2359.
- [18] T.W. Greene, *Protective Groups in Organic Synthesis*, third ed., John Wiley, New York, 1999.
- [19] Basicity calculated using MarvinSketch 4.1.5 software, Chemaxon Ltd. www.chemaxon.com/marvin.
- [20] K.H. Ahn, S.J. Lee, *Tetrahedron Lett.* 33 (1992) 507.
- [21] F. Abu-Hasanayn, T.J. Emge, J.A. Maguire, K. Krog-Jespersen, A.S. Goldman, *Organometallics* 13 (1994) 5177.